

1 Array design considerations for exploitation of stable
2 weakly dispersive modal pulses in the deep ocean

3 Ilya A. Udovydchenkov^a

4 ^a*Communication, Navigation and Sensor Signal Processing Department, Electronic*
5 *Systems and Technologies Technical Center, The MITRE Corporation, Bedford, MA,*
6 *01730, USA*

7 *and*

8 *Geology and Geophysics Department, Woods Hole Oceanographic Institution, Woods Hole*
9 *MA, 02543, USA*

10 **Abstract**

11 Modal pulses are broadband contributions to an acoustic wave field with
12 fixed mode number. Stable weakly dispersive modal pulses (SWDMPs) are
13 special modal pulses that are characterized by weak dispersion and weak
14 scattering-induced broadening and are thus suitable for communications ap-
15 plications. This paper investigates, using numerical simulations, receiver ar-
16 ray requirements for recovering information carried by SWDMPs under vari-
17 ous signal-to-noise ratio conditions without performing channel equalization.
18 Two groups of weakly dispersive modal pulses are common in typical mid-
19 latitude deep ocean environments: the lowest order modes (typically modes
20 1-3 at 75 Hz), and intermediate order modes whose waveguide invariant is
21 near-zero (often around mode 20 at 75 Hz). Information loss is quantified
22 by the bit error rate (BER) of a recovered binary phase-coded signal. With
23 fixed receiver depths, low BERs (less than 1%) are achieved at ranges up to
24 400 km with three hydrophones for mode 1 with 90% probability and with
25 34 hydrophones for mode 20 with 80% probability. With optimal receiver
26 depths, depending on propagation range, only a few, sometimes only two,
27 hydrophones are often sufficient for low BERs, even with intermediate mode
28 numbers. Full modal resolution is unnecessary to achieve low BERs. Thus, a
29 flexible receiver array of autonomous vehicles can outperform a cabled array.

30 *Keywords:*

31 Ocean acoustics, weakly dispersive modal pulses, long-range sound
32 propagation, underwater communications

33 **1. Introduction**

34 A broadband acoustic wave field can be represented as a superposition of
35 modal pulses [1, 2], which are broadband contributions to the wave field cor-
36 responding to fixed mode numbers. Stable weakly dispersive modal pulses
37 (SWDMPs) are special modal pulses that are characterized by negligible
38 dispersion and weak scattering-induced broadening. To appreciate the dif-
39 ference between SWDMPs and typical modal pulses, assume that the wave
40 field is excited by a point source whose time history consists of two cycles of
41 a carrier frequency. In that wave field the information carried by a SWDMP
42 is a delayed replica of the transmitted signal, two cycles of the carrier fre-
43 quency. In contrast, in the same wave field dispersion causes most other
44 (typical) modal pulses to unravel into frequency-modulated sweeps whose
45 duration grows with increasing range. The anomalous absence of unrav-
46 eling of the SWDMPs leads to potentially important underwater acoustic
47 communications applications. The received SWDMP waveform is to a good
48 approximation a replica of the transmitted signal, thereby eliminating (un-
49 der ideal circumstances) the need to equalize. The difference in behavior
50 between SWDMPs and typical modal pulses can be explained by the fact
51 that SWDMPs have the special property that the waveguide invariant for
52 that mode number, evaluated at (or very near) the center frequency, is equal
53 to zero. The extraction of a modal pulse, weakly dispersive or not, requires
54 mode filtering. This paper investigates, using theoretical arguments and
55 numerical simulations, the receiver array design requirements necessary to
56 extract, from an acoustic wave field, an accurate estimate of a SWDMP,
57 and, in turn, the information carried by it.

58 Simulations are performed in a nearly stratified ocean environment using
59 a typical mid-latitude sound speed profile, in which two groups of weakly
60 dispersive modal pulses commonly occur. The first group is the lowest or-
61 der modes (modes 1-3 at 75 Hz are considered in the paper). The second
62 group consists of intermediate order modes (around mode 20 at 75 Hz) whose
63 waveguide invariant is near-zero. Broadband acoustic wave fields are simu-
64 lated at ten equally spaced ranges between 50 km and 500 km with a point
65 source transmitting a phase-modulated binary sequence. The resulting wave
66 fields are mode processed using various receiver array configurations. The
67 modal pulses are demodulated to estimate the transmitted binary sequence.

68 Signal distortions lead to inter-symbol interference (ISI) and are quantified
69 by the bit error rate (BER) (the percentage of incorrectly detected bits),
70 which is a convenient measure of the performance. No a priori receiver train-
71 ing or channel equalization is performed. To estimate uncertainties due to
72 environmental variations, which in turn cause variations in the modal shapes,
73 all simulations and post-processing steps are repeated 10 times with different
74 realizations of the sound speed perturbation field.

75 One question that motivated this analysis is: Under what conditions can
76 the information carried by a SWDMP be recovered with small errors (as
77 measured by BERs) if the corresponding modes are not fully resolved? In
78 the environments considered in this paper, which closely resemble a typical
79 mid-latitude deep ocean sound speed profile, approximately 40 hydrophones
80 are needed to resolve the first 10 modes at 75 Hz [3–6]. It turns out that low
81 BERs can often be realized when the modes comprising a SWDMP are not
82 fully resolved. It is shown that, for the lowest order modes, a surprisingly
83 small number of hydrophones at fixed depths, sometimes as few as three,
84 is needed to achieve low BERs at ranges up to 400 km. For the SWDMPs
85 corresponding to modes 19 and 20 as few as 34 hydrophones at fixed depths
86 may be needed to achieve low BERs. It is also shown that only two or
87 four hydrophones may be sufficient to achieve low BERs for SWDMPs for
88 low and intermediate mode numbers, respectively, if the receiver depths are
89 optimally chosen depending on the horizontal distance to the source. Of
90 course, one cannot expect an adequate resolution of any modes with only
91 two hydrophones, or mode 20 at 75 Hz with only four hydrophones, but full
92 modal resolution turns out to be unnecessary to achieve low BERs. With
93 this analysis a portable and flexible receiver array composed of autonomous
94 underwater vehicles (AUVs) will, in some instances, have superior commu-
95 nications performance to cabled arrays.

96 Since SWDMPs experience little propagation-induced distortion, they are
97 useful in communications applications [7, 8]. The underwater acoustic chan-
98 nel is a challenging communications media due to the constantly fluctuating
99 ocean environment and due to multipath propagation which results in large
100 channel delay spread [9]. In a deep ocean long-range acoustic communication
101 system, a signal consisting of a sequence of symbols experiences significant
102 ISI (up to several seconds or hundreds of transmitted symbols [10]), which
103 precludes achieving reliable high-speed data transmissions. A common so-
104 lution is to design a receiver that compensates for the ISI and employs a
105 decision feedback equalizer (DFE) [9]. However, large channel delay spread

106 increases the complexity of the required DFE [11].

107 An important milestone in long-range underwater acoustic communica-
108 tions is the work of Freitag and Stojanovic [12]. The authors processed
109 the acoustic data transmitted over 3250 km range using an adaptive multi-
110 channel DFE with integrated phase tracking and Doppler compensation and
111 showed that the joint use of 20 hydrophones allowed near symbol-rate com-
112 munications (37.5 bps). At this long range the channel spread is on the order
113 of several seconds requiring many equalizer taps, but the computational com-
114 plexity is partially mitigated by the low symbol-rate.

115 It is demonstrated in this paper that the extraction of information car-
116 ried by SWDMPs prior to equalization reduces the channel delay spread by
117 exploiting the physics of the underwater sound channel and the properties of
118 the acoustic wave field, thus reducing the complexity of the DFE. Note that
119 mode processing differs from reduced complexity equalization. The latter is
120 designed to invert the distortions due to propagation through the channel.
121 The mode-processed wave field, however, is still a solution to the acoustic
122 wave equation. One possible extension of this analysis, which is outside of the
123 current scope, is to revisit the receiving array requirements if modal analysis
124 is combined with the equalization method presented in [12]. A disadvantage
125 to our approach is that SWDMPs might not exist in a given environment for
126 the ranges considered. While SWDMPs exist in many ocean environments,
127 they are not ubiquitous.

128 SWDMPs are related to weakly divergent beams [7]. Weakly divergent
129 beams were described theoretically in [13] and later in [14, 15] and they have
130 been observed experimentally in the North Atlantic at ranges up to 3500 km
131 [16–18] and in the Norwegian Sea at ranges up to 1000 km [19]. The connec-
132 tion between weakly divergent beams and SWDMPs arises from ray-mode
133 duality: the asymptotic equivalence of acoustic wave fields described using
134 rays or as a superposition of normal modes [20, 21]. Here we demonstrate
135 that information carried by SWDMPs, even corresponding to intermediate
136 mode numbers, can be recovered with a few hydrophones with their positions
137 well-predicted by the asymptotic ray-mode duality results.

138 The remainder of the paper is organized as follows. Section II provides
139 an example demonstrating that only two hydrophones could be sufficient to
140 extract the information carried by a SWDMP corresponding to an intermedi-
141 ate order mode at 400 km range. Section III describes numerical simulations
142 of acoustic wave fields and the processing algorithm used to estimate BERs.
143 Section IV is divided into three subsections and presents the results relating

144 to low order modes, to intermediate order modes, and to processing with min-
 145 imal arrays. Minimal arrays have the fewest number of elements to achieve a
 146 given BER threshold, and the hydrophone depths are allowed to vary depend-
 147 ing on the source-receiver distance. It is shown that full modal resolution
 148 is unnecessary to achieve low BERs. It is demonstrated that the optimal
 149 hydrophone depths can be well predicted using mode rays (rays whose ac-
 150 tion variable is determined by the quantization condition [2]) corresponding
 151 to the SWDMPs. The dependence of array requirements on signal-to-noise
 152 ratio (SNR) is also analyzed. Discussion of the results is presented in Section
 153 V. Conclusions are given in Section VI.

154 2. Motivating example: Why are SWDMPs special?

155 Two slightly different range-independent ocean sound speed profiles are
 156 considered in this paper. These profiles are shown in Figure 1. The first
 157 profile, called C0, is the canonical “Munk” mid-latitude ocean profile [22].
 158 The second profile, C1, is the same as C0 with a Gaussian disturbance added
 159 in the upper ocean [23]. C1 qualitatively resembles an environment con-
 160 structed from the hydrographic data in the Eastern North Pacific ocean [24].
 161 The C0 profile can be thought of as a generic mid-latitude deep ocean sound
 162 speed profile for which low order modes are expected to be weakly disper-
 163 sive. The C1 profile supports SWDMPs corresponding to intermediate order
 164 modes. This expectation is illustrated in the right panel of Figure 1, which
 165 shows the dependence of the waveguide invariant β [25, 26] on mode num-
 166 ber at 75 Hz for both profiles. The theory of modal group time spreads
 167 [2, 6, 26, 27] predicts that the modal dispersion is largely controlled by the
 168 product $I(m, f)\beta(m, f)$, where I is the ray action, f is acoustic frequency,
 169 and m is the mode number. It follows from the asymptotic quantization
 170 condition (see, for example, Eq. (3) in [6]) that the ray action grows lin-
 171 early with the mode number. Thus, in the C0 profile only modes with small
 172 I -values (low order modes) are weakly dispersive. However, the C1 profile
 173 also supports an intermediate range of mode numbers around $m = 20$ with
 174 near-zero β , which are also expected to be weakly dispersive.

175 It turns out that low BERs can often be achieved in a binary transmission
 176 with a non-mode-resolving receiving array without channel equalization, if
 177 one focuses on SWDMPs. To illustrate this observation consider the example
 178 shown in Figure 2 (the choice of simulation parameters is explained in Ap-
 179 pendix A). Assume a typical stratified mid-latitude deep ocean environment

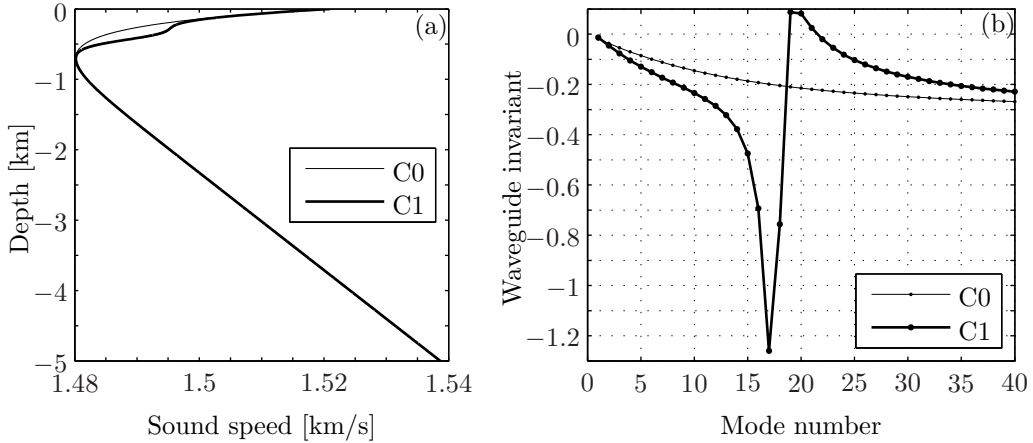


Figure 1: a) Two background sound-speed profiles considered in this paper: C0 is the canonical “Munk” profile and C1 is the same as C0 with a Gaussian disturbance added in the upper ocean. b) Waveguide invariant β at 75 Hz versus mode number in C0 and in C1.

180 with the background sound speed profile C1 shown in the left panel of Fig-
 181 ure 1, on which a range- and depth-dependent sound speed perturbation due,
 182 for example, to internal waves (IWs) is superimposed. An acoustic source
 183 placed at 190 m depth transmits 1 binary digit which consists of 2 cycles of
 184 a phase-modulated signal with a 75 Hz carrier frequency. Figure 2a) shows
 185 the source function. Figures 2b) and 2c) show modal pulses corresponding
 186 to modes 20 and 30, respectively, at the source. Figure 2d) illustrates the
 187 mode 30 pulse arrival at 250 km range filtered using a dense receiving array.
 188 Significant pulse broadening and distortions are observed due to dispersion
 189 and scattering. Figure 2e) shows the mode 20 pulse at 250 km range fil-
 190 tered using the same dense receiving array. Unlike the mode 30 pulse, the
 191 shape of the mode 20 pulse is almost unchanged. The estimated shape of the
 192 mode 20 pulse obtained using only two hydrophones placed at 710 m and 740
 193 m depths is shown in Figure 2f). While modal “cross-talk” is unavoidable
 194 in this example, the “cross-talk” does not prevent one from correctly esti-
 195 mating the modal arrival. In fact, in this example, BERs are zero in 7 out
 196 of 10 simulations with different realizations of the IW-induced sound speed
 197 perturbation field.

198 It is shown in Section IV that with the source transmitting a sequence
 199 of binary digits, even with SNR as low as 5 dB, the optimal placement of a

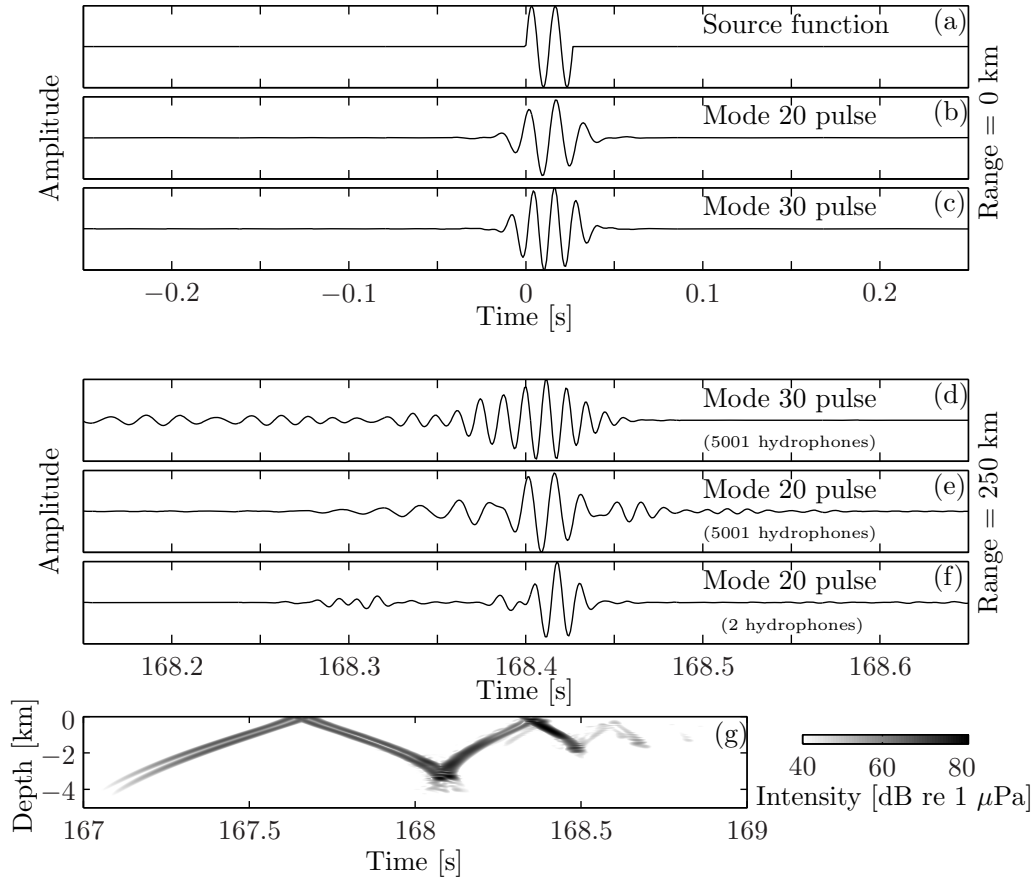


Figure 2: Evolution of the mode 20 and mode 30 pulses from the source to 250 km range. a) The source function showing one binary digit that consists of two cycles of the carrier frequency at 75 Hz. b) The mode 20 pulse at the source. c) The mode 30 pulse at the source. d) The mode 30 pulse at 250 km range filtered using 5001 hydrophones with 1 m spacing. e) The mode 20 pulse at 250 km range filtered using 5001 hydrophones with 1 m spacing. f) The mode 20 pulse at 250 km range processed using two hydrophones at 710 m and 740 m depth. All amplitudes are normalized to unity, except the mode 20 pulse amplitude at the source (b), which is normalized to the peak amplitude of the mode 30 pulse (c) to show that the mode 30 pulse is excited slightly stronger than the mode 20 pulse. g) The wave field intensity versus arrival time and depth at 250 km range produced by a point source placed at 190 m depth that transmits 1 binary digit.

200 few hydrophones often results in low BERs. In contrast, BERs are always
201 high for the mode 30 pulse, even with high SNR and a dense receiving array
202 covering the entire water column. So, how is it possible that BERs for some
203 modal pulses are small or even zero with a non-mode-resolving array, while
204 for other modal pulses even a dense mode-resolving array covering the entire
205 water column results in high BERs? The large differences between Figures
206 2d) and 2e) (or 2d) and 2f)) arise because SWDMPs (the mode 20 pulse in
207 this example) are special: they experience almost no distortion due to disper-
208 sion and scattering along the propagation path. Also, similarities between
209 Figures 2e) and 2f) suggest that perfect modal resolution is unnecessary to
210 correctly identify digits, and only a few hydrophones could be sufficient. This
211 paper investigates the design of a communications system that takes the most
212 advantage of the special properties of SWDMPs in the deep ocean.

213 It is important to note that the receiving array geometry and the source
214 depth in this motivating example are chosen to efficiently excite the mode 20
215 pulse, which propagates in the C1 environment to long ranges with minimal
216 distortion. The results of these considerations can also be illustrated by
217 plotting the wave field intensity versus arrival time and depth as shown in
218 Figure 2g), which is an approximation to the underwater channel impulse
219 response (the impulse in this case is 1 binary digit consisting of 2 cycles of the
220 carrier frequency). The energy corresponding to the mode 20 pulse appears as
221 a contribution to the high intensity arrival with small time spread at around
222 168.42 s. Note, however, that if one does not focus on the minimally spread
223 mode 20 pulse, the receiver has to compensate for the propagation-induced
224 distortions in that high intensity arrival and for other distorted arrivals.

225 These studies are also motivated by results from the Long-range Ocean
226 Acoustic Propagation EXperiment (LOAPEX) [28, 29]. It was shown, using
227 these experimental data [8], that low order mode SWDMPs propagate in
228 the Eastern North Pacific ocean without significant distortions up to 500
229 km range. In that experiment, a vertical line array of hydrophones with 40
230 elements was used. The array covered depths between approximately 350
231 m and 1750 m with 35 m spacing between hydrophones. Unfortunately,
232 that array did not resolve mode numbers higher than approximately 10.
233 Thus, it was not possible to utilize SWDMPs corresponding to intermediate
234 mode numbers. Numerical simulations presented here address this issue and
235 estimate the least number of hydrophones needed for low BERs with either
236 low or intermediate order SWDMPs.

237 **3. Numerical simulations. Acoustic propagation modeling and post-**
238 **processing of simulated wave fields**

239 Numerically simulated wave fields are constructed using the range-dependent
240 acoustic propagation model RAM [30, 31]. The details are summarized in
241 Appendix A. These wave fields have been compared with the wave fields
242 computed using a split-step Fourier PE model [32] and excellent agreement
243 was observed.

244 Figure 3 shows an example of the simulated acoustic wave field and the
245 corresponding mode 1 arrival at 500 km range in the C0 profile with the
246 IW-induced perturbation superimposed. The point source is placed at 800
247 m depth (the same depth that was used in LOAPEX). Figure 3a) shows the
248 wave field intensity as a function of depth and time resulting from a 1023-digit
249 m -sequence transmission. Figure 3b) shows the wave field in panel (a) after
250 pulse compression. Figures 3c) and 3d) show the mode 1 arrival, obtained
251 from the wave fields in the corresponding top panels, before pulse compression
252 and after pulse compression, respectively. To quantify the dependence of
253 BERs on SNR we consider the wave field before pulse compression, such as
254 shown in Figure 3a) and simulate ambient noise as uniformly distributed in
255 depth and in time with levels relative to the highest rms signal pressure level
256 over depth. For computational feasibility, four levels of SNR are considered:
257 5, 10, 15, and 20 dB. The LOAPEX data analysis (not discussed in this paper)
258 suggests that these element-level SNR values are realistic at propagation
259 ranges up to 500 km, though a more powerful source might be needed to
260 achieve the highest 20 dB SNR at 500 km range. While this noise model
261 might be considered an oversimplification, it is adequate to demonstrate the
262 usefulness of the SWDMPs. More complex data-driven noise models would be
263 needed to accurately account for the spatial correlation properties of the noise
264 field. The simulated wave fields are obtained at ten equally spaced ranges
265 between 50 km and 500 km in both profiles, C0 and C1, with the IW-induced
266 perturbations superimposed. To reduce computational complexity only 10
267 different realizations of the IW-induced perturbation fields are considered.
268 Thus, the probability of achieving a certain BER with a given array geometry
269 is estimated in 10% increments.

270 Now the post-processing steps of the simulated wave fields, such as shown
271 in Figure 3a), are discussed. From the analysis of the LOAPEX data [8]
272 modes 1-3 are expected to be weakly dispersive in a canonical profile, so we
273 focus on these modes first.

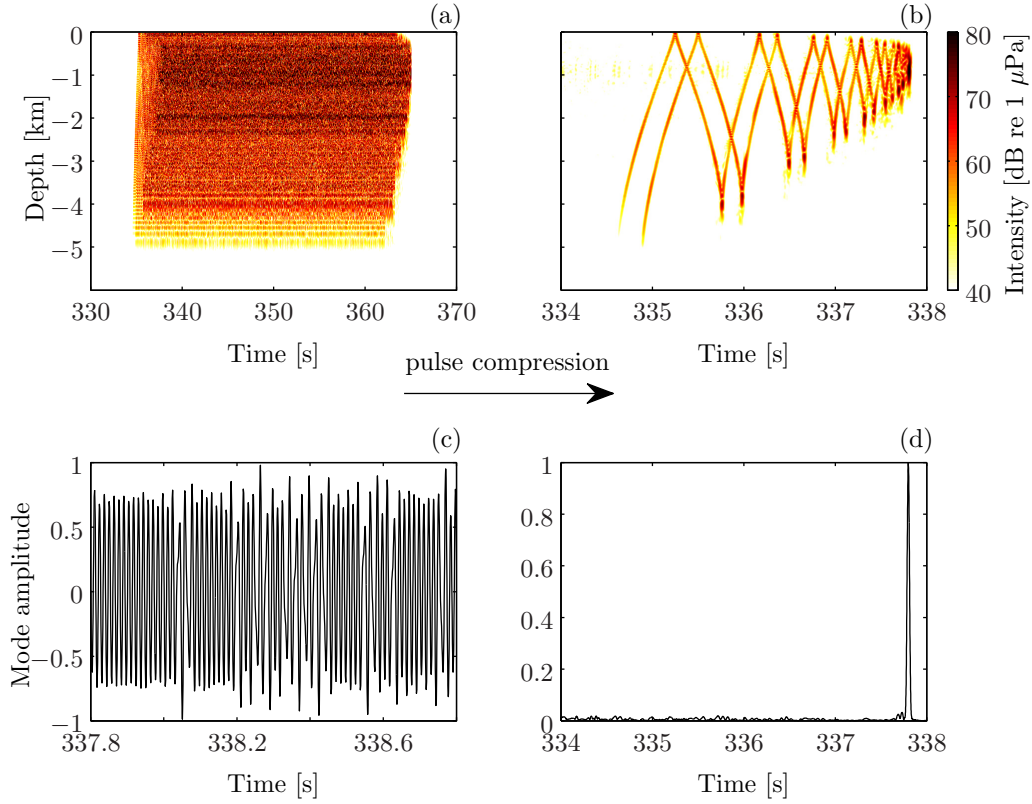


Figure 3: (Color online). The broadband acoustic wave field and the mode 1 arrival simulated at 500 km range in the C0 profile with the IW-induced perturbation superimposed. a) The wave field intensity versus arrival time and depth before pulse compression produced by a point source at 800 m depth with the 75 Hz carrier frequency emitting a phase-modulated m -sequence. b) The wave field in (a) after pulse compression (matched filtering). c) The mode 1 arrival of the mode-processed wave field shown in (a). d) The mode 1 arrival after pulse compression. Note that the mode 1 arrival in (d) may be obtained either by pulse compression of the mode 1 arrival in (c), or by mode filtering of the wave field in (b). The mode filtering was performed with a long and dense array sufficient to resolve all propagating modes.

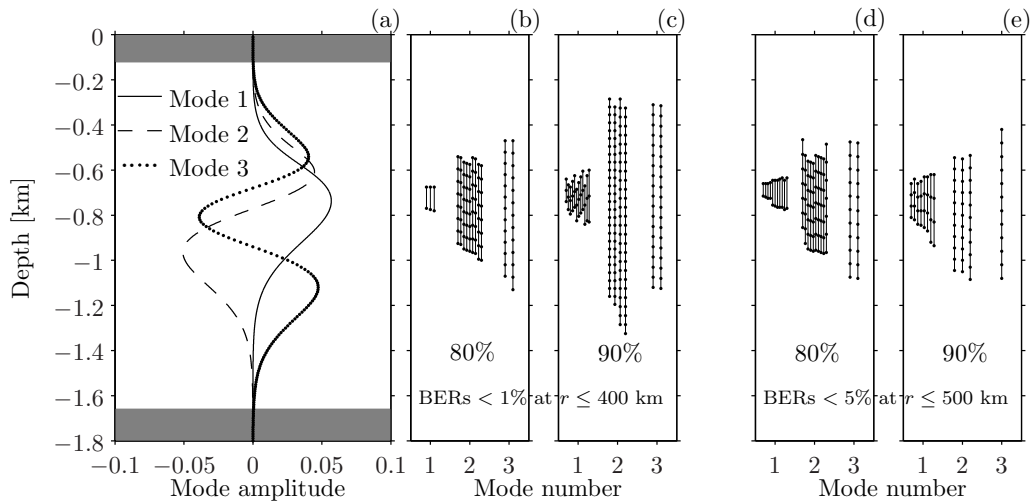


Figure 4: a) Modes 1, 2, and 3 computed at 37.5 Hz in the C0 profile. The domain of interest lies between 120 m and 1660 m (unshaded area). b) Array configurations resulting in BERs of less than 1% with 80% probability, at all eight ranges simultaneously up to 400 km, from processing of modes 1, 2, and 3 with a simulated SNR=20 dB. c) Array configurations resulting in BERs of less than 1% with 90% probability, at all eight ranges simultaneously up to 400 km, from processing of modes 1, 2, and 3 with a simulated SNR=20 dB. d) Same as panel (b), but with BERs of less than 5% at ten ranges up to 500 km. e) Same as panel (c), but with BERs of less than 5% at ten ranges up to 500 km. Note that the mode numbers are integers and the array configurations are offset horizontally from the integer marks for visualization purposes.

274 It is computationally prohibitive to test all possible receiving array config-
 275 urations, so some simplifications are made. The lowest frequency of interest,
 276 37.5 Hz, is chosen as the first null in the spectrum of the m -sequence mod-
 277 ulated with two cycles of the 75 Hz carrier per digit (see Appendix A). The
 278 depth domain in which the mode 3 amplitude at this frequency is negligi-
 279 ble (less than 40 dB below its peak value) is truncated as shown in Figure
 280 4a) by gray shaded areas. The remaining test depths are between 120 m
 281 and 1660 m. Each tested array is uniquely defined by three parameters: the
 282 number of hydrophones, the separation between hydrophones, and the depth
 283 of the shallowest hydrophone. The minimum hydrophone separation is 5 m.
 284 The separation increment is also 5 m (only arrays with equal hydrophone
 285 separations of 5 m, 10 m, 15 m, etc. are tested). The depth-step for the
 286 shallowest hydrophones is also 5 m. The number of hydrophones in a test
 287 array varies between 2 and 309. For the low mode number analysis, a to-
 288 tal of 257,292 arrays are tested. More details describing the selected array
 289 configurations are given in Appendix B.

290 To quantify the performance of these arrays the wave fields are mode
 291 processed and demodulated. The details of the demodulation are explained
 292 in Section III in [8]. To extract the binary sequence from carrier-modulated
 293 modal amplitudes $a_m(t)$ the following procedure was used. First, the signal
 294 was bandpass filtered between 50 and 100 Hz and then complex demodulated
 295 to baseband. Instantaneous phase $Y_m(t)$ and envelope signal $A_m(t)$ time
 296 series were computed for each transmission using a zero-phase forward-and-
 297 reverse 5-th order lowpass Butterworth filter [33, 34]. Discrete samples of
 298 the phase $Y_m(t)$ (sampled at 1200 Hz) were grouped into bins containing 32
 299 samples (one digit is two cycles of the carrier; in the signal sampled at 16
 300 times the carrier one digit contains 32 samples), and values within each bin
 301 were averaged. Because the transmitted sequence was a binary sequence, only
 302 the sign was retained after averaging. (For convenience we shall refer to the
 303 bits as + and - bits, corresponding to the sign of the phase modulation angle
 304 of the transmitted binary sequence.) Binary sequences derived from each
 305 transmission for each m -value were compared with the transmitted sequence
 306 bit-by-bit. The BER is the fraction (often expressed as a percentage) of the
 307 1023 transmitted bits that are incorrectly identified. The zero-crossings of
 308 $Y_m(t)$ identify the times at which the phase polarity of successive incoming
 309 digits is reversed. The number of samples between any two zero-crossings
 310 should be a multiple of 32.

311 To implement this algorithm one needs to synchronize the incoming signal

312 with the binary sequence. In other words, it is necessary to find the reference
 313 point in time at which a digit begins. Two considerations need to be taken
 314 into account. First, it is necessary to know how to group samples into bins of
 315 32, i.e., to identify which of the 32 samples is the closest to the beginning of
 316 the digit. This can be accomplished by circular shifting the received signal
 317 by k samples, where k is an integer between 0 and 31. In practice one also
 318 needs to make sure that the synchronization time is not off by more than one
 319 digit, so in the actual implementation we varied k between -32 and 64. The
 320 second problem is to synchronize the initial phase, because the beginning
 321 of a digit, in general, does not coincide with a sampling point. This can
 322 be accomplished by shifting the phase of the signal by φ_0 , which can vary
 323 between $-\pi$ and π . We did not attempt to find an efficient method to
 324 estimate k and φ_0 (which likely can be done from an analysis of incoming
 325 receptions). Instead, a brute force search that minimizes BERs of the signal
 326 recorded with a mode-resolving array was implemented to determine k and
 327 φ_0 for each $a_m(t)$.

328 Many of the array configurations tested are not mode resolving and do
 329 not allow accurate estimation of modal amplitudes and phases. Here discrete
 330 direct projection [4, 5, 35] is used no matter how sparse or short the test array
 331 is (even with only two elements). This processing results in modal “cross-
 332 talk”. However, such analysis is still useful if one focuses on SWDMPs and
 333 one is only interested in finding phase transitions between the received digits.
 334 We refer to this analysis as “mode processing” as opposed to “mode filtering”
 335 (as shown in Figure 3), where the array is sufficiently long and dense to
 336 isolate individual modes. This mode processing can also be thought of as a
 337 computation of a weighted sum of received signals with modal eigenfunction
 338 values at the receiver depths.

339 4. Results

340 4.1. Low order modes

341 First, we focus on low order modes and the simulations performed in
 342 the C0 background profile with the IW-induced perturbation superimposed.
 343 Since the transmitted signal is known, one can compute BERs for all possible
 344 array configurations. Figures 4b) and 4c) show array configurations with the
 345 smallest number of hydrophones that resulted in BERs of less than 1% after
 346 processing modes 1-3 with all hydrophone depths fixed *at all eight ranges*
 347 *simultaneously up to 400 km*. Figure 4b) shows arrays that achieve BERs of

348 less than 1% with 80% probability (in 8 out of 10 realizations). Figure 4c)
349 shows arrays that achieve the desired BERs with 90% probability. Figures
350 4d) and 4e) are constructed similarly, except that the desired BER threshold
351 is relaxed to 5% and the propagation range is extended to 500 km (the ranges
352 of 450 km and 500 km were included). Only a subset of all configurations is
353 shown for mode 1 in Figures 4c), 4d), and 4e).

354 These simulations show that two hydrophones are sufficient to achieve
355 BERs of less than 1% with 80% probability by processing mode 1 at ranges
356 up to 400 km. The number of required hydrophones is larger for modes 2 and
357 3 if BERs of less than 1% are desired. However, only 7-12 hydrophones are
358 sufficient with mode 2 (or 3) processing at ranges up to 500 km to achieve
359 BERs of less than 5% with 80% (or 90%) probability, provided the SNR is
360 high (20 dB).

361 Several interesting conclusions can be made from Figure 4. First, a re-
362 markably small number of hydrophones (2-4) are needed to achieve low BERs
363 by processing mode 1 at ranges up to 500 km. This is a consequence of
364 the simple mode 1 shape in depth. Second, Figure 4c) suggests that mode
365 2 processing could require more hydrophones than mode 3 to achieve low
366 BERs. This is a consequence of the energy redistribution among modes due
367 to scattering along the propagation path. At some intermediate ranges the
368 amplitude of mode 2 (as computed with the fully mode-resolving array) is
369 significantly lower than the amplitude of modes 1 or 3. In Figure 4c) the
370 amplitude of mode 2 is low at some range in two or more realizations of the
371 IW-induced perturbation field. Consequently, BERs of less than 1% with
372 90% success are difficult to achieve and a long array (35 hydrophones) is re-
373 quired to overcome low SNR. (Do not confuse this SNR, which is estimated
374 from the mode amplitude, with the SNR used to simulate the acoustic wave
375 fields, defined in Section III). Thus, the variations of modal energy along the
376 propagation path are important. Third, the hydrophone spacing in arrays
377 resulting in low BERs varies between 50 m and 135 m for mode 1, between
378 35 m and 80 m for mode 2, and between 45 m and 60 m for mode 3. In all
379 cases the spacing is equal to a few wavelengths at 75 Hz, but is small enough
380 to sample the mode shape structure. Finally, the array configuration corre-
381 sponding to mode 3 shown in Figure 4e) does not span the depth aperture
382 of mode 3. It is clear that the array is not mode resolving yet the weighted
383 sum of contributions from mode 3 is sufficient to achieve low BERs.

384 One important objective of this work is to study the array requirements
385 depending on SNR. Acoustic wave fields with different SNR levels are simu-

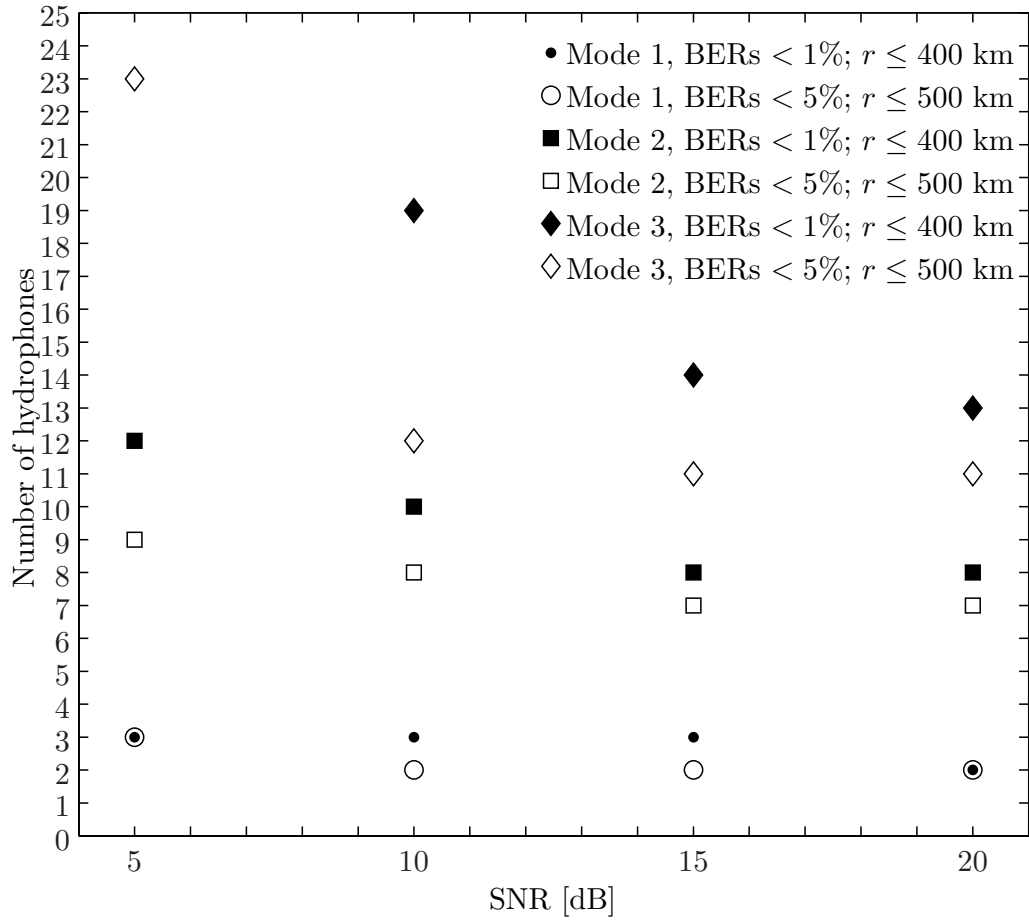


Figure 5: The number of hydrophones required to achieve either BERs of less than 1% at ranges up to 400 km or BERs of less than 5% at ranges up to 500 km with 80% probability by processing modes 1-3 for various SNRs. Sixty-three hydrophones are required to achieve BERs < 1% at $r \leq 400$ km by processing mode 3 with an SNR of 5 dB (not shown).

386 lated as explained in Section III. The least number of hydrophones required
387 to achieve BERs of less than 1% at ranges up to 400 km or BERs of less
388 than 5% at ranges up to 500 km with 80% probability for each SNR value
389 is shown in Figure 5 for modes 1-3. At an SNR of 20 dB these results are
390 consistent with Figures 4b) and 4d). With decreasing SNR, the number of
391 required hydrophones increases, as expected. However, the mode processing
392 results of mode 1 are so robust, that even with an SNR of 5 dB low BERs can
393 be achieved with just three hydrophones at all ranges. As expected, mode 1
394 results are the most stable among the three modes because of the simplest
395 structure of the mode 1 shape function in depth.

396 *4.2. Intermediate order modes with a near-zero waveguide invariant*

397 In this section the results obtained in the C1 background profile with IW-
398 induced perturbations superimposed are summarized. The focus here is on
399 intermediate mode numbers, for which the absolute value of the waveguide
400 invariant is close to zero, and their utility as SWDMPs.

401 It is necessary to emphasize an important distinction between low order
402 modes and intermediate order modes. To excite low order modes the source
403 depth should be near the sound channel axis. Then all low order modes are
404 excited, except those having a null at the source depth. This is suboptimal,
405 however, for the excitation of intermediate order modes. First, one needs to
406 choose which mode numbers to excite. The right panel of Figure 1 suggests
407 that modes between approximately 19 and 23 might be weakly dispersive,
408 because the corresponding values of the waveguide invariant β are close to
409 0. Strong excitation of mode 19 might not be desirable, however, because
410 energy can scatter into adjacent modes (18, 17, etc.) along the propagation
411 path, which are not weakly dispersive and have large negative values of β .
412 The energy then scatters back into mode 19 and the modal pulse spreads in
413 time. Since it is impossible to excite only one mode with a point source, it
414 is better to “change” the source depth towards exciting higher order modes.
415 A way to estimate an optimal source depth is shown in Figure 6. This figure
416 shows the dependence of the waveguide invariant β on frequency for modes
417 19 and 20 constructed using the asymptotic quantization condition [26]. It
418 is desirable to excite modes at those frequencies for which β is close to 0.

419 To estimate the source depth an arbitrary threshold of 0.15 is chosen and
420 the frequency bands within which $|\beta| < 0.15$ are selected for mode numbers
421 19 and 20. The source depth of 190 m is computed as the mean value of
422 the upper turning points (first nulls of the second derivative of the modal

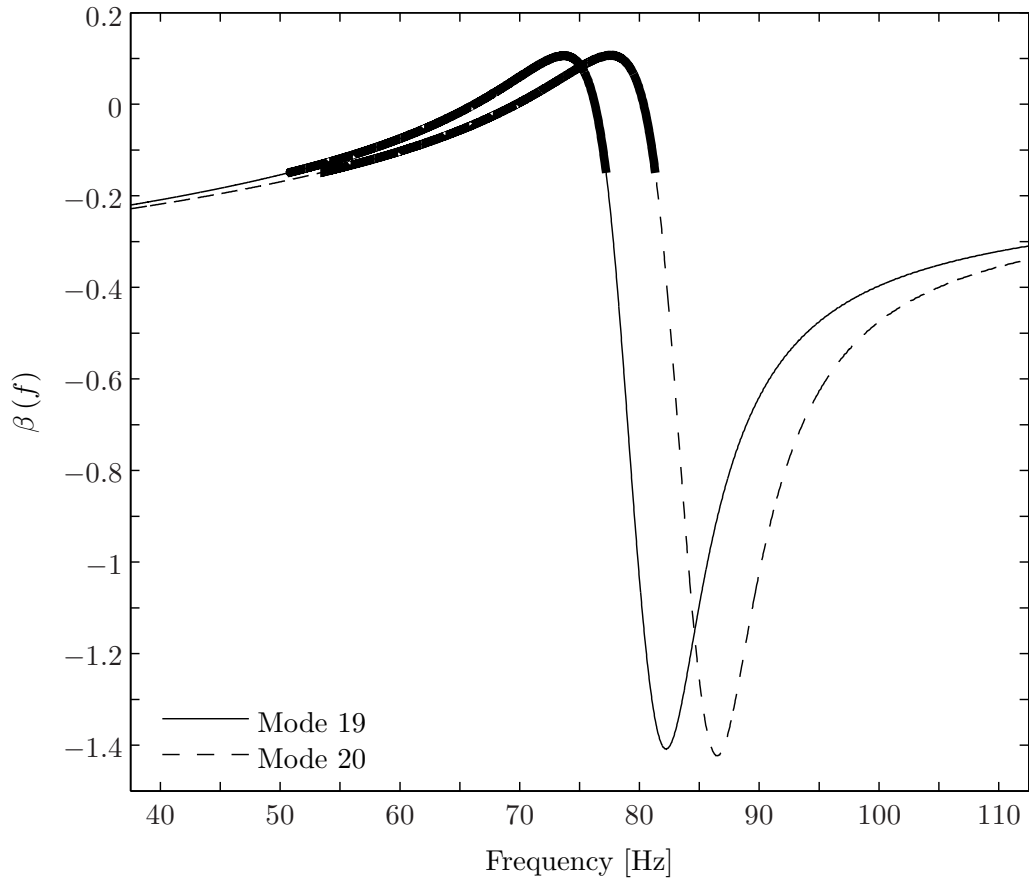


Figure 6: The waveguide invariant (β) dependence on frequency for modes 19 and 20. The frequency bands within which $|\beta| < 0.15$ are shown in bold. The source should be placed at a depth where it will excite modes at these frequencies. The estimated optimal source depth is 190 m.

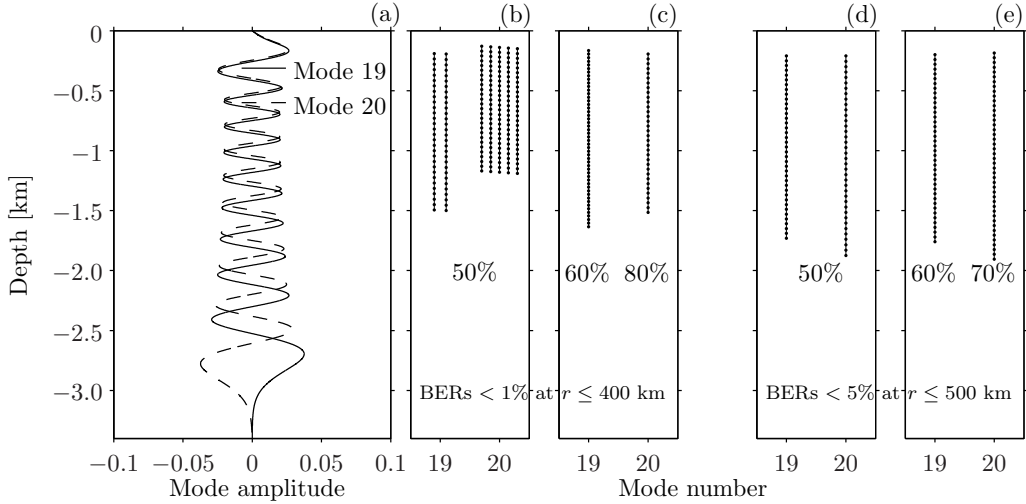


Figure 7: a) Modes 19 and 20 computed at 37.5 Hz in the C1 profile. The domain of interest is between the ocean surface and 3400 m depth. b-e) Arrays that resulted in BERs not exceeding a given threshold (1% or 5%) at ranges up to 400 km or 500 km with respective probabilities. These panels are constructed similarly to Figures 4b)-4e).

423 shape functions) of modes 19 and 20. Variations of the threshold imposed
 424 on $|\beta|$ showed little sensitivity in the source depth estimate. A set of full
 425 wave numerical simulations with a full water column array is performed with
 426 source depths around 190 m to confirm the lowest BERs for modes 19 and
 427 20 at long ranges.

428 The analysis for modal pulses corresponding to modes 19 and 20 is similar
 429 to the analysis for low order modes. The spacing model between hydrophones
 430 is the same as for low order modes, but the maximum number of hydrophones
 431 in the tested arrays is increased to cover a depth aperture of 3400 m resulting
 432 in a total of 1,432,727 combinations.

433 Figure 7 is constructed similarly to Figure 4. However, the probabilities
 434 of achieving the desired BERs are lowered from 80% and 90% to the values
 435 between 50% and 80%. In all cases the arrays resulting in low BERs do not
 436 span the mode aperture of either mode 19 or 20. Despite the finer structure of
 437 modes 19 and 20 in depth, the separation between hydrophones that results
 438 in low BERs is between 30 m and 45 m, which is again a few wavelengths.

439 This analysis shows that low BERs are still achieved at ranges up to 400
 440 km provided SNR is sufficiently high. Figure 8 shows the number of hy-
 441 drophones required to achieve low BERs for modes 19 and 20 versus SNR.

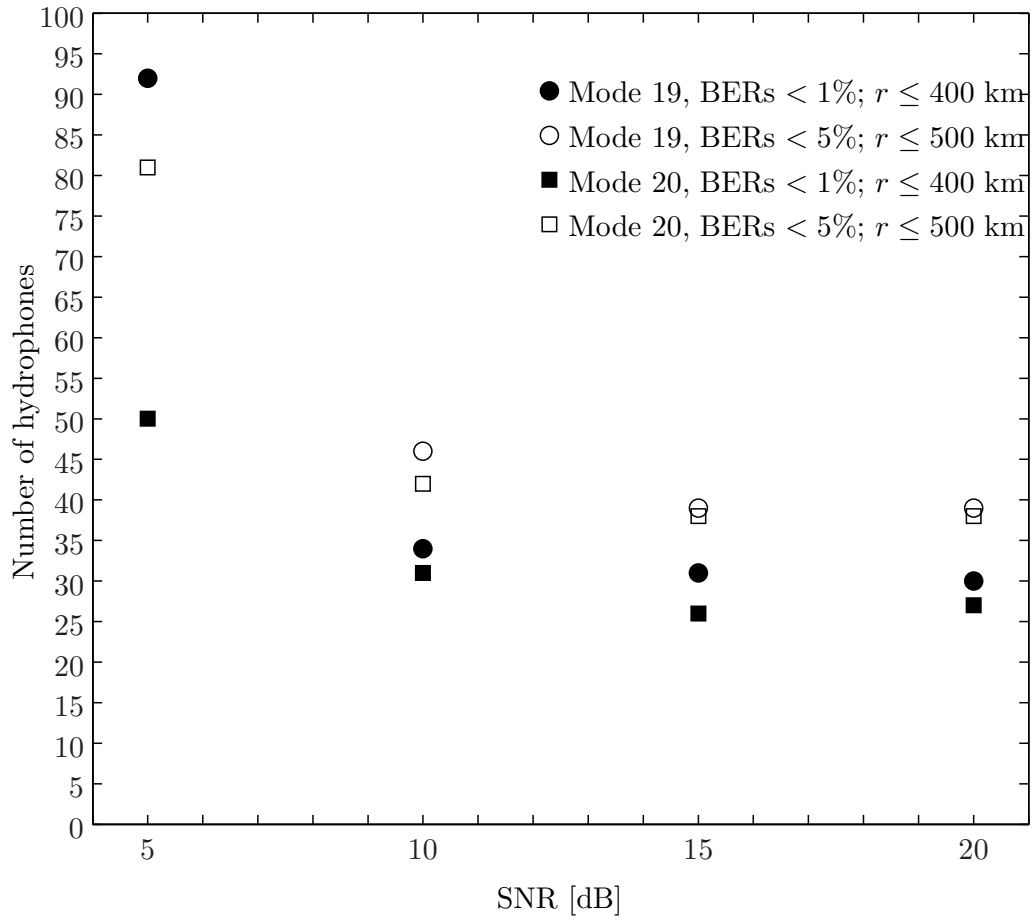


Figure 8: The number of hydrophones required to achieve either BERs of less than 1% at ranges up to 400 km or BERs of less than 5% at ranges up to 500 km with 50% probability using processing of modes 19 and 20 for various SNRs. One hundred and fifty-eight hydrophones are required to achieve BERs < 5% at $r \leq 500$ km by processing mode 19 with an SNR of 5 dB (not shown).

Table 1: The least number of hydrophones, at optimal receiver depths, required to achieve BERs of less than 1% at ranges up to 400 km as a function of mode number and SNR. Three values in each cell of the table correspond to the probabilities of 50%, 80%, and 90%. The infinity symbol means that no arrays satisfy the desired criteria.

C0					C1				
(a)					(b)				
Mode number \ SNR [dB]	20	15	10	5	Mode number \ SNR [dB]	20	15	10	5
1	2,2,2	2,2,2	2,2,2	2,2,3	19	4,13, ∞	4,13, ∞	6,17, ∞	9,58, ∞
2	2,5,9	2,5,9	2,6,10	2,11,25	20	3,12,17	4,12,20	4,14,28	6,23,83
3	4,11,15	5,13,19	6,15,50	9,36, ∞					

442 Approximately 30 hydrophones are needed for either mode 19 or 20, if the
 443 depths of the hydrophones are fixed for all eight source-receiver ranges up to
 444 400 km. The required number of hydrophones increases rapidly with SNR
 445 falling below approximately 10 dB. Overall, these results are promising, as
 446 they demonstrate that the required number of hydrophones for achieving low
 447 BERs is smaller than one initially expects (several hydrophones per wave-
 448 length).

449 4.3. Mode processing with minimal arrays

450 Only a few hydrophones are often sufficient to achieve low BERs for
 451 either low or intermediate order modes, if the depths of the hydrophones on
 452 the test array are not restricted to be the same for all transmission ranges.
 453 The performance of such a system and its limitations are discussed in this
 454 section.

455 Table 1 shows the least number of hydrophones required to achieve BERs
 456 of less than 1% at ranges up to 400 km as a function of mode number and
 457 SNR. The three values in each cell of the table correspond to the probabilities
 458 of 50%, 80%, and 90%. Two hydrophones are sufficient with mode 1 pro-
 459 cessing for almost any SNR and desirable success rate. Generally, among the
 460 first 3 modes (Table 1a)), the number of required hydrophones increases with
 461 increasing mode number and decreasing SNR. The results re-emphasize the
 462 conclusion that energy redistribution among modes along the propagation
 463 path is important. This is why the number of required hydrophones rapidly
 464 increases at low SNRs for the 90% success rate.

465 Surprisingly, only a few hydrophones are required to achieve low BERs
 466 with SWDMPs corresponding to modes 19 and 20 (Table 1b)). Even with

467 the lowest SNR of 5 dB, the number of required hydrophones is less than 10,
468 provided the desirable success rate is not too high (50% in this case). Only 3
469 hydrophones are sufficient for a mode 20 pulse if the SNR is high. One should
470 not be confused, however, regarding the “50% success rate” of the system.
471 The success rate of 50% means that in half of the transmissions BERs at the
472 receiver, decoding a 1023-digit sequence, are less than 1% (or 5% in some
473 examples discussed above), and another half of the transmissions had errors
474 greater than 1%. This, of course, *does not* mean that 50% of the transmitted
475 information is decoded incorrectly. A practical advantage of this analysis is
476 that systems with a few hydrophones are easier to deploy and operate, so
477 the reduced success rate is a reasonable trade-off between performance and
478 feasibility.

479 The dependence of BERs on the number of hydrophones in the receiv-
480 ing array is complex. Depending on environmental conditions and source
481 and receiver depths one might achieve low BERs without equalization even
482 with a single hydrophone. This typically occurs if the propagation range is
483 sufficiently short. In this case, obviously, there is no benefit from modal anal-
484 ysis. As propagation range increases, it is beneficial to increase the number
485 of receivers to estimate the desired SWDMP more accurately. It is difficult
486 to predict, however, how much improvement, if any, would be achieved if a
487 single hydrophone or a few hydrophones are added to an existing system.

488 As an example, consider an array consisting of 3 hydrophones at 590 m,
489 650 m, and 710 m depths in the C0 environment. Processing of mode 1 with
490 this array at 500 km propagation range results in BERs of less than 1% in
491 9 out of 10 simulations (i.e. with 90% probability). With any subset of this
492 array, the chance of achieving BERs of less than 1% does not exceed 60%.
493 So, in this example an addition of the third hydrophone to the existing 2-
494 hydrophone array increases the chance of reception at 500 km with less than
495 1% BER from 60% to 90%. Unfortunately, it is computationally intractable
496 task to quantify in general the significance of adding an extra hydrophone to
497 an existing array of an arbitrary length and configuration.

498 How does one find the depths of hydrophones that result in low BERs?
499 While there is no simple rule that guarantees that desired positions can be
500 found without prior measurements of the wave field, some guidelines can be
501 offered. These guidelines are based on the results shown in Figure 9. In this
502 figure two mode numbers are considered: mode 1 in the C0 profile, shown in
503 Figure 9a), and mode 20 in the C1 profile, shown in Figure 9c). The SNR
504 level was 10 dB. All two-hydrophone arrays that resulted in BERs of less

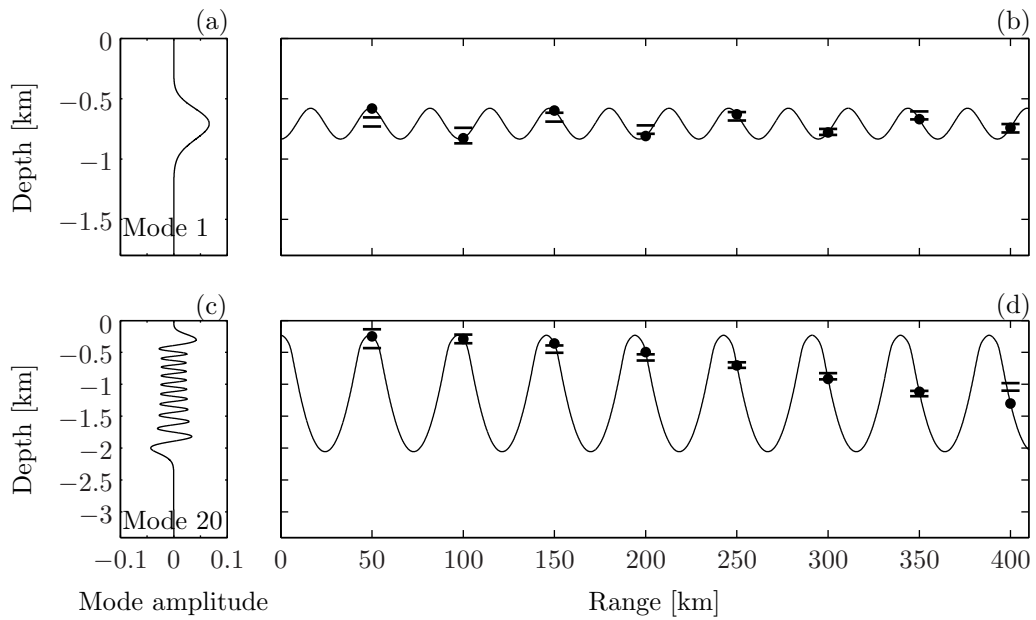


Figure 9: Estimating hydrophone depth for low BERs. a) Mode 1 in the C0 profile at 75 Hz. b) Depth estimates for two-hydrophone arrays that resulted in BERs of less than 1% with an SNR of 10 dB and a probability of 90%. c) Mode 20 in the C1 profile at 75 Hz. d) Depth estimates for four-hydrophone arrays that resulted in BERs of less than 1% for an SNR of 10 dB and a probability of 50%. Corresponding mode rays are shown by solid lines. The depths of mode rays at the discrete ranges of interest are shown by black dots.

505 than 1% for mode 1 at ranges up to 400 km with a probability of 90% are
506 found. In this case there are a total of 3,700 arrays at 50 km and only 1
507 array at 300 km. It was observed that at some ranges only one hydrophone
508 is sufficient to correctly decode the transmitted digits. This observation
509 is not surprising at short ranges for which propagation-induced distortions
510 are insignificant. At longer ranges good BERs could sometimes be achieved
511 with only one hydrophone as well, but this behavior is not expected to be
512 robust. The explanation is likely linked to the dependence of the SWDMP
513 amplitude (and thus SNR) on propagation range. While on average (over
514 many realizations of the perturbation field) the amplitude of a modal pulse
515 is expected to monotonically decrease with range, this dependence might not
516 be monotonic for a particular realization of the perturbation field resulting
517 in clearer arrivals at longer ranges. To estimate the most likely placement
518 of a desirable array, the mean depth and one standard deviation in depth of
519 all hydrophones are computed at each range. The resulting two depth values
520 (mean \pm one standard deviation) for mode 1 processing are shown by short
521 tick marks at each range in Figure 9b). The same analysis is repeated for
522 mode 20, except that four-hydrophone arrays are considered and the desired
523 success rate is lowered to 50%. The results are shown in Figure 9d).

524 To explain the observed pattern two mode rays are computed. The mode
525 ray shown in Figure 9b) starts at the lower turning point of mode 1 (834 m),
526 the mode ray shown in Figure 9d) starts at the average depth of the upper
527 turning points for modes 19 and 20 at 75 Hz (231 m). The selection of the
528 up- and down-going mode ray depends on the depth of the source relative
529 to the turning point of the mode (an up-going ray is chosen for mode 1, and
530 a down-going ray is chosen for mode 20). Recall that the arrays considered
531 here are not mode resolving. The “cross-talk” between modes 19 and 20
532 observed with the four-hydrophone arrays is large. This is why the ray with
533 the starting depth at the average turning depths of modes 19 and 20 agrees
534 better with predicted array depths than the mode 20 mode ray. Overall, the
535 agreement between array predictions based on full wave simulations and ray
536 theory is very good for both modes 1 and 20. For mode 1 the agreement is
537 slightly worse at short ranges suggesting that the source should be placed
538 closer to the peak in the mode shape function, rather than along the mode
539 ray.

540 It is also interesting to compare the phases of modal arrivals estimated
541 with these short arrays to the correct phases estimated through mode filtering
542 with the full water column array (with 5001 hydrophones). Figure 10 shows

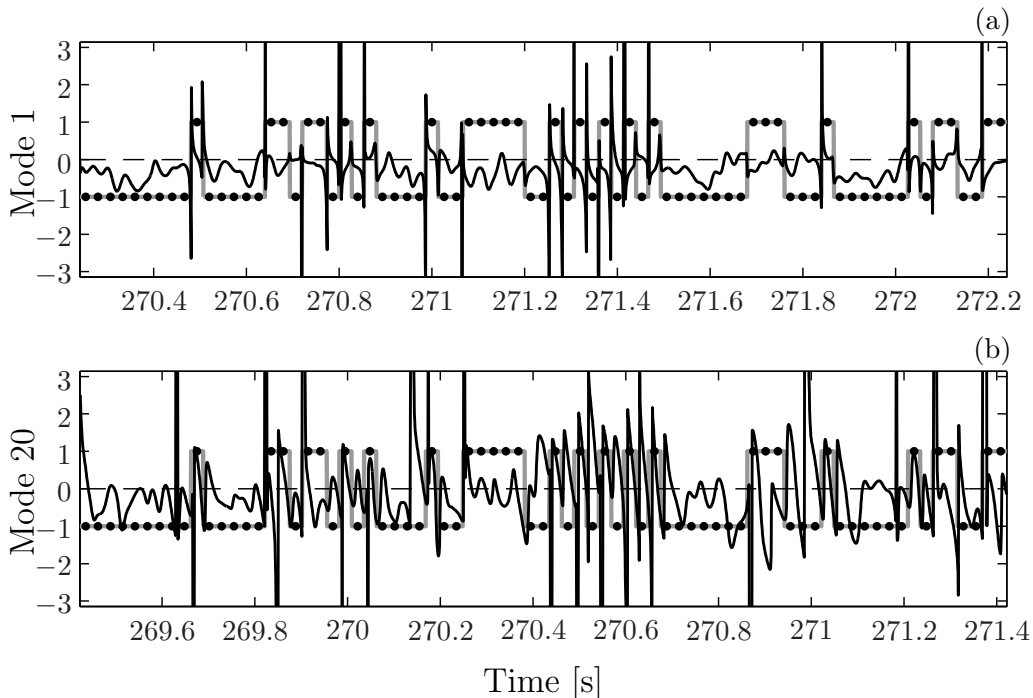


Figure 10: An example of phase errors from two-hydrophone array processing for mode 1 (top panel) and four-hydrophone array processing for mode 20 (bottom panel) at 400 km range with an SNR of 10 dB. The phase errors are shown with black solid lines. The thick gray line is the idealized transmitted square wave (with unit amplitude). The black dots show the digits recovered from the phase function. The horizontal axis is the absolute arrival time. The vertical axis on each panel shows phase errors between $-\pi$ and π .

543 phase errors with black lines for mode 1 (top panel) and mode 20 (bottom
 544 panel) at 400 km range with an SNR of 10 dB. The time axis under each
 545 subplot shows the absolute arrival time. Thus, the mode 20 pulse arrives
 546 approximately 0.8 s earlier than the mode 1 pulse at 400 km range. Despite
 547 fairly large phase errors, phase transitions are identified correctly, and the
 548 transmitted binary sequence is recovered without errors for mode 1, and with
 549 BERs of less than 1% for mode 20 (there are no errors in the first 75 digits
 550 shown in the bottom panel of Figure 10) .

551 Finally, note that while the results are sensitive to the variations of
 552 modal amplitude along the propagation path due to scattering, the modal
 553 pulse spreads do not change significantly for different realizations of the IW-
 554 induced perturbation field as long as the IW model is valid (i.e. the pertur-

555 bation statistics are adequately described by the Garrett-Munk spectrum).
556 This can be seen from theoretical arguments and numerical simulations pre-
557 sented in earlier work. The performance of the system relying on SWDMP in
558 terms of BERs is largely controlled by the total time spread for that modal
559 pulse, which is described by Eq. (6) (or its variations) in [6]. The two
560 constituents of Eq. (6), the reciprocal bandwidth contribution, and the de-
561 terministic dispersive contribution (Eqs. (7) and (8) in [6], respectively) do
562 not depend on the properties or the statistics of the internal waves. The third
563 term, Eq. (9) in [6], depends only on the strength of the IW-induced pertur-
564 bation field through the parameter B (do not confuse it with the thermocline
565 depth discussed in Appendix A), which does not depend on a particular re-
566 alization. Thus, the total time spread variations of the modal pulse (and
567 consequently expected BER variations) are statistically insignificant as long
568 as the strength of the IW-induced fluctuations (and B) remains unchanged
569 (1 nominal Garrett-Munk strength (GM) was used in all simulations). Quan-
570 titatively, time spreads may change in environments with different perturba-
571 tion strength, but variations due to a particular realization are insignificant.
572 Note, however, that the results are sensitive to the amplitude fluctuations
573 of modal pulses along the propagation path, which are caused by scattering
574 due to internal waves.

575 5. Discussion

576 The results presented here are expected to be useful in communications
577 applications. Focusing on SWDMPs prior to channel equalization signifi-
578 cantly reduces the channel delay spread thus decreasing the complexity of
579 the required equalization scheme. The efficient use of SWDMPs with a mod-
580 est number of receivers and optimal source placement could potentially be
581 exploited for communications between moving platforms. The knowledge of
582 the longest range that the signal propagates undistorted is also important
583 for underwater communications.

584 This paper explains, using theoretical arguments and numerical simula-
585 tions, how to design a long-range acoustic underwater system in the deep
586 ocean that takes advantage of the special properties of SWDMPs. Two
587 groups of SWDMPs are considered in typical mid-latitude ocean environ-
588 ments: those that correspond to low order modes (modes 1-3 at 75 Hz), and
589 those corresponding to intermediate order modes, for which the waveguide
590 invariant parameter is near-zero (19 and 20 at 75 Hz). It is shown that

591 SWDMPs corresponding to modes 1-3 may be useful in communications ap-
592 plications at ranges up to 500 km, which is consistent with the results of the
593 LOAPEX data analysis [8]. For longer ranges one should take into account
594 the mesoscale variability and variations of the background sound speed pro-
595 file along the propagation path. SWDMPs corresponding to intermediate
596 mode numbers are expected to be observable at ranges up to 400 km. There
597 are two reasons that these modes do not perform as well as low order modes.
598 The first reason is the scattering from nearby strongly dispersive modes in
599 the vicinity of modes 19 and 20 (modes 15-18, for example). This scattering
600 may cause the arrivals for modes 19 and 20 to spread. The second reason
601 is the variation of the IW-induced fluctuation strength with depth, that is
602 expressed through the parameter $B(m)$ and which increases approximately
603 linearly with mode number (see Section V in [26] for the discussion of the
604 $B(m)$ dependence). Nevertheless, both groups of weakly dispersive modes
605 are expected to be observable at ranges of several hundreds of kilometers.

606 This paper shows that only a small number of hydrophones may be
607 needed to achieve low BERs without channel equalization. With fixed re-
608 ceiver depths and at the ten ranges considered (between 50 km and 500 km)
609 only 4 hydrophones are needed to achieve BERs of less than 5% using mode
610 1, 11 using mode 2, and 12 using mode 3 for all propagation distances pro-
611 vided SNR is up to 20 dB with 90% probability. For intermediate mode
612 numbers (modes 19 and 20) around 30 hydrophones are needed. In either
613 case the receiving array does not need to span the entire mode shape in
614 depth. However, one needs to ensure that modal “cross-talk” caused by a
615 short and sparse receiving array does not inhibit the demodulation algorithm
616 from detecting the phase transitions. The guidelines for estimating optimal
617 source depth are offered, which could be useful if one desires to operate a
618 shallow source.

619 It is also shown that if the depths of the hydrophones are allowed to vary
620 depending on the source-receiver distance, often only two hydrophones are
621 sufficient to achieve low BERs with SWDMPs corresponding to either low
622 order modes and three or four hydrophones could be sufficient if intermediate
623 mode numbers are used. This would be important in a practical design if one
624 desires to use navigated autonomous vehicles or a mooring with adjustable
625 hydrophone depths instead of a fixed array installation. The estimates are
626 reliable with either group of modes at ranges up to 400 km. The desirable
627 depths of hydrophones are well predicted by ray theory with some caveats as
628 mentioned above.

629 The number of hydrophones required to achieve low BERs rapidly in-
630 creases as SNR decreases below approximately 10 dB. However, the LOAPEX
631 data analysis demonstrated that desired SNRs could be achieved at ranges
632 up to 500 km. Unfortunately, it does not seem feasible to derive simple
633 analytical expressions for the dependencies of BERs on SNR. The resulting
634 BERs depend on many factors besides the SNR, such as the distribution of
635 acoustic energy in the water column and across the receiving array, the sig-
636 nal coherence across individual elements, the distribution of energy among
637 modes, and the amount of modal cross-talk. These characteristics, in turn,
638 depend on the environmental conditions, source and receiver geometries, and
639 propagation range. Therefore, BERs in this paper are estimated numerically
640 under various conditions.

641 The results presented in this paper rely on the assumption that the sound
642 speed profile is approximated as a range-independent background profile with
643 small range- and depth-dependent IW-induced perturbations superimposed.
644 In environments with strong range dependence, however, similar analysis can
645 be carried out. The results also rely on the accuracy of the 2D acoustic propa-
646 gation model RAM. In environments with significant out-of-plane scattering,
647 bottom reflections, or horizontal refraction this analysis should be revisited.
648 Also note that while SWDMPs (or corresponding weakly divergent beams)
649 were observed in some environments, they are not expected to be ubiqui-
650 tous. A comprehensive analysis of the existence and practical usefulness of
651 SWDMPs in various environments would be necessary.

652 **6. Conclusions**

653 This paper demonstrates the potential utility of SWDMPs for long-range
654 underwater data transmission. It is shown that both groups of weakly disper-
655 sive modal pulses that commonly occur in typical mid-latitude deep ocean
656 environments, the lowest order modes and the intermediate order modes
657 whose waveguide invariant is near-zero, can be used at ranges up to 500
658 km. The guidelines for estimating the optimal source depth are provided.
659 This paper also demonstrates that full modal resolution is unnecessary to
660 accurately recover the information carried by SWDMPs. Therefore the re-
661 quirements on the extent and the number of hydrophones in the receiving
662 array are greatly reduced. The necessary depths of hydrophones are well
663 predicted by acoustic ray theory.

Table A.1: Summary of the parameters used in the numerical model.

C_1 [km/s]	z_1 [km]	B [km]	ε	dc [km/s]
1.48	-0.7	0.52	0.0025	0.008
z_c [km]	z_w [km]	h [km]	ρ_w, ρ_s [kg/m ³]	h_s [m]
-0.35	0.1	5	1000	1000
c_s [km/s]	α_1 [dB/ λ]	α_2 [dB/ λ]	SL [dB]	f_{min} [Hz]
1538.67	0.05	0.35	195	37.5
f_{max} [Hz]	Δr [km]	Δz [km]	n_p	r_s [km]
112.5	0.1	0.001	4	50

664 **Acknowledgments**

665 The author thanks Dr. Ralph Stephen for proofreading the manuscript.
 666 The author thanks Dr. Michael Brown and Dr. Oleg Godin for valuable
 667 suggestions and recommendations. The author also thanks Dr. Timothy
 668 Duda and Dr. Ying-Tsong Lin for the PE-based numerical model used for
 669 comparison and validation of the simulated wave fields. This research did not
 670 receive any specific grant from funding agencies in the public, commercial,
 671 or not-for-profit sectors.

672 **Appendix A.**

673 Details of the RAM-code numerical simulations and the choice of relevant
 674 parameters are presented in this appendix. Two slightly different range-
 675 independent ocean sound-speed profiles are considered. The first profile,
 676 called C0, is the canonical ‘‘Munk’’ mid-latitude ocean profile. The second
 677 profile, called C1 in this paper, is the same as in [23] and is a perturbed
 678 version of C0.

679 All parameters of the numerical model are summarized in Table A.1. In
 680 C0, using the original ‘‘Munk’’ profile notation, C_1 is the sound speed at the
 681 sound channel axis, z_1 is the depth of the axis, B is the thermocline depth
 682 scale, and ε is a dimensionless constant. In the perturbed profile, $c_M(z)$ is
 683 the canonical ‘‘Munk’’ profile, dc is the maximum amplitude of the Gaussian
 684 perturbation, z_c is the depth of the midpoint of the Gaussian perturbation,
 685 and z_w is the width of the Gaussian perturbation. Additional environmental
 686 parameters are h , the depth of the ocean (assumed constant), ρ_w and ρ_s ,

687 densities of the water and sediment, respectively, c_s , the compressional speed
688 of the sediment, set equal to the water sound speed at the water/sediment
689 interface, h_s , the sediment thickness, α_1 and α_2 , compressional attenuations
690 at the top and the bottom of the sediment layer (with a linear gradient
691 assumed in between). Acoustic parameters are source level, SL, plus f_{min}
692 and f_{max} , the lowest and highest frequencies of interest. Computational
693 scheme parameters are the range step Δr , the depth step Δz , the number
694 of Padé terms n_p , and the range r_s (from the source) where the stability
695 constraint is turned off.

696 While it was previously shown that bottom reflections could interfere
697 with purely water column refracted energy at short transmission ranges [36],
698 bottom reflections are neglected in this modeling. Bottom properties in the
699 model are set to suppress these reflections. The IW-induced sound-speed per-
700 turbations are modeled using the procedure described by [37]. The strength
701 of the IW-induced perturbations is one nominal Garret-Munk strength (1
702 GM).

703 The acoustic source is a phase-modulated m -sequence at 75 Hz, with
704 1023-digits and each digit corresponds to two cycles of the carrier frequency.
705 The m -sequence is the same as in LOAPEX [28]. The total duration of the
706 source signal, T_0 , is 27.28 sec. The resulting spectrum is broadband with the
707 maximum near 75 Hz, and the first nulls, f_{min} and f_{max} , near 37.5 and 112.5
708 Hz.

709 It is important to note a few subtleties in the construction of the analyzed
710 wave fields, an example of which is shown in Figure 3. To fit the entire
711 reception into the model time window at long ranges, the window must be
712 longer than T_0 . The window length is given by the inverse of the frequency
713 spacing. The selection of 4,092 computed frequencies covering $f_{max} - f_{min}$
714 (75 Hz), gives a sufficient window length of $2T_0$. Therefore, the actual source
715 function used in simulations consisted of the 27.28 s signal and an equally
716 long period of silence. It is well known that this type of source function is
717 not compatible with optimal two-state correlation processing of m -sequences
718 to estimate impulse response (i.e. arrivals shown in Figures 3b) and 3d). To
719 analyze a pulse-compressed signal with a source function duration of $2T_0$, the
720 source signal should consist of exactly two periods of the m -sequence. This is
721 unnecessary here, however, because the objective is to analyze modal arrivals
722 *before* pulse compression, with no attention paid to special properties of the
723 m -sequences. The only consequence of the chosen T_0 -length source function
724 is the presence of energy leakage across time (temporal sidelobes) in both

725 Figures 3b) and 3d). These pulse-compressed arrivals, however, are shown
726 for illustration purposes only and are not further analyzed. Note that the
727 same 4,092 frequencies were used for the computation of normal modes and
728 for the mode filtering. Modes were computed using the KRAKEN normal
729 mode code [38].

730 Appendix B.

731 The details describing the selected array configurations are presented in
732 this appendix. Two sets of receiving arrays are considered in this paper:
733 one in C0 and the other in C1 environments. The main difference between
734 the two sets is that they span different depth apertures. All considered
735 hydrophones are placed between $h_1 = 120$ m and $h_2 = 1660$ m depths in C0
736 and between $h_1 = 0$ m and $h_2 = 3400$ m depths in C1. In both environments
737 the minimum hydrophone separation, the separation increment, and the the
738 depth-step for the shallowest hydrophone are the same and equal to $\Delta h = 5$
739 m. The number of hydrophones in all tested arrays varies between 2 and
740 the maximum number that fits into the depth aperture with the minimum
741 separation, i.e. $(1660-120)/5+1=309$ in C0 and $(3400-0)/5+1=681$ in C1.
742 The total number of 2-element arrays is

$$\begin{aligned} & \frac{h_2 - h_1}{\Delta h} + \left(\frac{h_2 - h_1}{\Delta h} - 1 \right) + \left(\frac{h_2 - h_1}{\Delta h} - 2 \right) + \dots + \left(\frac{h_2 - h_1}{\Delta h} - \left(\frac{h_2 - h_1}{\Delta h} - 1 \right) \right) = \\ & \frac{h_2 - h_1}{2\Delta h} \times \left(\frac{h_2 - h_1}{\Delta h} + 1 \right), \end{aligned} \quad (\text{B1})$$

743 which is 47,586 in C0 and 231,540 in C1. The total number of 3-element
744 arrays is

$$\left(\frac{h_2 - h_1}{\Delta h} - 1 \right) + \left(\frac{h_2 - h_1}{\Delta h} - 3 \right) + \dots + \left(\frac{h_2 - h_1}{\Delta h} - \left(\frac{h_2 - h_1}{\Delta h} - 1 \right) \right) = \left(\frac{h_2 - h_1}{2\Delta h} \right)^2, \quad (\text{B2})$$

745 which is 23,716 in C0 and 115,600 in C1. In general, the total number of
746 k -element arrays is

$$\sum_j \left(\frac{h_2 - h_1}{\Delta h} - (j \times (k - 1) - 1) \right), \quad (\text{B3})$$

747 where the sum is taken over all such integer j 's that result in all terms
748 under the summation being positive. It is easy to confirm numerically that
749 the total number of arrays considered is 257,292 in C0 and 1,432,727 in C1
750 environments.

751 **References**

- 752 [1] A. L. Virovlyansky, Ray theory of long-range sound propagation in the
753 ocean, Institute of Applied Physics, Nizhny Novgorod, Russia (in Rus-
754 sian), 2006.
- 755 [2] A. L. Virovlyansky, A. Y. Kazarova, L. Y. Lyubavin, Ray-based descrip-
756 tion of normal modes in a deep ocean acoustic waveguide, *Journal of the*
757 *Acoustical Society of America* 125 (2009) 1362–1373.
- 758 [3] K. E. Wage, Broadband modal coherence and beamforming at megame-
759 ter ranges, Ph.D. thesis, Massachusetts Institute of Technology (2000).
- 760 [4] K. E. Wage, A. B. Baggeroer, J. C. Preisig, Modal analysis of broadband
761 acoustic receptions at 3515-km range in the North Pacific using short-
762 time Fourier techniques, *Journal of the Acoustical Society of America*
763 113 (2003) 801–817.
- 764 [5] K. E. Wage, M. A. Dzieciuch, P. F. Worcester, B. M. Howe, J. A. Mer-
765 cer, Mode coherence at megameter ranges in the North Pacific Ocean,
766 *Journal of the Acoustical Society of America* 117 (2005) 1565–1581.
- 767 [6] I. A. Udovydchenkov, M. G. Brown, T. F. Duda, J. A. Mercer, R. K.
768 Andrew, P. F. Worcester, M. A. Dzieciuch, B. M. Howe, J. A. Colosi,
769 Modal analysis of the range evolution of broadband wavefields in the
770 North Pacific Ocean: Low mode numbers, *Journal of the Acoustical*
771 *Society of America* 131 (2012) 4409–4427.
- 772 [7] M. G. Brown, I. A. Udovydchenkov, Underwater communication using
773 weakly dispersive modal pulses, *Acoustical Physics* 59 (2013) 533–538.
- 774 [8] I. A. Udovydchenkov, M. G. Brown, T. F. Duda, P. F. Worcester, M. A.
775 Dzieciuch, J. A. Mercer, R. K. Andrew, B. M. Howe, J. A. Colosi,
776 Weakly dispersive modal pulse propagation in the North Pacific ocean,
777 *Journal of the Acoustical Society of America* 134 (2013) 3386–3394.

- 778 [9] M. Stojanovic, J. A. Catipovic, J. G. Proakis, Reduced-complexity spa-
779 tial and temporal processing of underwater acoustic communication sig-
780 nals, *Journal of the Acoustical Society of America* 98 (1995) 961–972.
- 781 [10] H. C. Song, B. M. Howe, M. G. Brown, R. K. Andrew, Diversity-based
782 acoustic communication with a glider in deep water, *Journal of the*
783 *Acoustical Society of America* 135 (2014) 1023–1026.
- 784 [11] A. Song, M. Badiy, H. C. Song, W. S. Hodgkiss, M. B. Porter,
785 the KauaiEx Group, Impact of ocean variability on coherent underwa-
786 ter acoustic communications during the Kauai experiment (KauaiEx),
787 *Journal of the Acoustical Society of America* 123 (2008) 856–865.
- 788 [12] L. Freitag, M. Stojanovic, Basin-scale acoustic communication: a fea-
789 sibility study using tomography m-sequences, *OCEANS, MTS/IEEE*
790 *Conference and Exhibition 4* (2001) 2256 – 2261.
- 791 [13] S. D. Chuprov, Selection of modes and rays in underwater sound chan-
792 nels, in: *Acoustics of the Ocean Medium*, Nauka, Moscow (in Russian),
793 1989, pp. 56–64.
- 794 [14] Y. V. Petukhov, A sound beam with minimal wavefront divergence in a
795 stratified ocean waveguide, *Acoustical Physics* 40 (1994) 97–105.
- 796 [15] Y. V. Petukhov, Slowly-diverging acoustics beams in smoothly inhom-
797 geneous ocean waveguides, *Acoustical Physics* 43 (1997) 196–201.
- 798 [16] L. M. Brekhovskikh, V. V. Goncharov, S. A. Dremuchev, V. M.
799 Kurtepov, V. G. Selivanov, Y. A. Chepurin, Long range sound propaga-
800 tion experiment in the Canarian Abyssal Plain, the Atlantic, *Acoustical*
801 *Physics* 36 (1990) 824–831.
- 802 [17] L. M. Brekhovskikh, V. V. Goncharov, V. M. Kurtepov, Weakly diver-
803 gent bundles of rays and their possible use in inverse methods of ocean
804 acoustics, in: *Full field inversion methods in ocean and seismo-acoustics*,
805 *Kluwer Academic Publishers*, Dordrecht, Netherlands, 1995, pp. 39–44.
- 806 [18] L. M. Brekhovskikh, V. V. Goncharov, V. M. Kurtepov, Weakly di-
807 vergent bundles of sound rays in the Arctic, *Atmospheric and Oceanic*
808 *Physics* 31 (1995) 441–446.

- 809 [19] V. V. Goncharov, V. M. Kurteпов, Formation and propagation of weakly
810 diverging bundles of rays in a horizontally inhomogeneous ocean, *Acous-
811 tical Physics* 40 (1994) 685–692.
- 812 [20] M. G. Brown, F. J. Beron-Vera, I. Rypina, I. A. Udovydchenkov, Rays,
813 modes, wavefield structure, and wavefield stability, *Journal of the Acous-
814 tical Society of America* 117 (2005) 1607–1610.
- 815 [21] F. J. Beron-Vera, M. G. Brown, Underwater acoustic beam dynamics,
816 *Journal of the Acoustical Society of America* 126 (2009) 80–91.
- 817 [22] W. H. Munk, Sound channel in an exponentially stratified ocean with
818 application to SOFAR, *Journal of the Acoustical Society of America* 55
819 (1974) 220–226.
- 820 [23] I. I. Rypina, I. A. Udovydchenkov, M. G. Brown, A transformation of
821 the environment eliminates parabolic equation phase errors, *Journal of
822 the Acoustical Society of America* 120 (2006) 1295–1304.
- 823 [24] R. A. Stephen, P. F. Worcester, I. A. Udovydchenkov, E. Aaron, S. T.
824 Bolmer, S. Carey, S. P. McPeak, S. A. Swift, M. A. Dzieciuch, Cruise
825 report: Ocean Bottom Seismometer Augmentation in the North Pacific
826 (OBSANP), Tech. Rep. WHOI-2014-03, Woods Hole Oceanographic In-
827 stitution, Woods Hole, MA (2014).
- 828 [25] S. D. Chuprov, Interference structure of a sound field in a layered ocean,
829 *Ocean Acoustics, Current State*, (1982) 71–91.
- 830 [26] I. A. Udovydchenkov, M. G. Brown, Modal group time spreads in weakly
831 range-dependent deep ocean environments, *Journal of the Acoustical
832 Society of America* 123 (2008) 41–50.
- 833 [27] D. Makarov, S. Prants, A. L. Virovlyansky, G. Zaslavsky, *Ray and wave
834 chaos in ocean acoustics*, World Scientific, Hackensack, New Jersey,
835 USA, 2010, p. 389 pages.
- 836 [28] J. A. Mercer, R. K. Andrew, B. M. Howe, J. A. Colosi, Cruise re-
837 port: Long-range ocean acoustic propagation experiment (LOAPEX),
838 Tech. Rep. APL-UW TR0501, Applied Physics Laboratory, University
839 of Washington, Seattle, WA (2005).

- 840 [29] J. A. Mercer, J. A. Colosi, B. M. Howe, M. A. Dzieciuch, R. Stephen,
841 P. F. Worcester, LOAPEX: The Long-Range Ocean Acoustic Propaga-
842 tion EXperiment, *IEEE Journal of Oceanic Engineering* 34 (2009) 1–11.
- 843 [30] M. D. Collins, E. K. Westwood, A higher-order energy-conserving
844 parabolic equation for range-dependent ocean depth, sound speed and
845 density, *Journal of the Acoustical Society of America* 89 (1991) 1068–
846 1075.
- 847 [31] M. Collins, A split-step Padé solution for the parabolic equation method,
848 *Journal of the Acoustical Society of America* 93 (1993) 1736–1742.
- 849 [32] Y.-T. Lin, T. F. Duda, A. E. Newhall, Three-dimensional sound propa-
850 gation models using the parabolic-equation approximation and the split-
851 step Fourier method, *Journal of Computational Acoustics* 21 (2013)
852 1250018–1–1250018–24.
- 853 [33] T. W. Parks, C. S. Burrus, *Digital Filter Design*, John Wiley and Sons,
854 Inc., New York, New York, 1987, Ch. 7, pp. 161–171, 213–218.
- 855 [34] A. Oppenheim, R. W. Schaffer, J. R. Buck, *Discrete-Time Signal Pro-
856 cessing*, Prentice-Hall, Inc., Upper Saddle River, New Jersey, 1999, Ch.
857 5.6, pp. pp. 280–291.
- 858 [35] J. R. Buck, J. C. Preisig, K. E. Wage, A unified framework for mode
859 filtering and the maximum a posteriori mode filter, *Journal of the Acous-
860 tical Society of America* 103 (1998) 1813–1824.
- 861 [36] I. A. Udovydchenkov, R. A. Stephen, T. F. Duda, S. T. Bolmer, P. F.
862 Worcester, M. A. Dzieciuch, J. A. Mercer, R. K. Andrew, B. M. Howe,
863 Bottom interacting sound at 50 km range in a deep ocean environment,
864 *Journal of the Acoustical Society of America* 132 (2012) 2224–2231.
- 865 [37] J. A. Colosi, M. G. Brown, Efficient numerical simulation of stochastic
866 internal-wave-induced sound speed perturbation fields, *Journal of the
867 Acoustical Society of America* 103 (1998) 2232–2235.
- 868 [38] M. B. Porter, The KRAKEN normal mode program. rep. sm-245, Tech.
869 rep., SACLANT Undersea Research Centre, La Spezia, Italy (1991).

870 **List of Figures**

871 1 a) Two background sound-speed profiles considered in this pa-
872 per: C0 is the canonical “Munk” profile and C1 is the same
873 as C0 with a Gaussian disturbance added in the upper ocean.
874 b) Waveguide invariant β at 75 Hz versus mode number in C0
875 and in C1. 6

876 2 Evolution of the mode 20 and mode 30 pulses from the source
877 to 250 km range. a) The source function showing one binary
878 digit that consists of two cycles of the carrier frequency at 75
879 Hz. b) The mode 20 pulse at the source. c) The mode 30
880 pulse at the source. d) The mode 30 pulse at 250 km range
881 filtered using 5001 hydrophones with 1 m spacing. e) The
882 mode 20 pulse at 250 km range filtered using 5001 hydrophones
883 with 1 m spacing. f) The mode 20 pulse at 250 km range
884 processed using two hydrophones at 710 m and 740 m depth.
885 All amplitudes are normalized to unity, except the mode 20
886 pulse amplitude at the source (b), which is normalized to the
887 peak amplitude of the mode 30 pulse (c) to show that the mode
888 30 pulse is excited slightly stronger than the mode 20 pulse. g)
889 The wave field intensity versus arrival time and depth at 250
890 km range produced by a point source placed at 190 m depth
891 that transmits 1 binary digit. 7

892 3 (Color online). The broadband acoustic wave field and the
893 mode 1 arrival simulated at 500 km range in the C0 profile with
894 the IW-induced perturbation superimposed. a) The wave field
895 intensity versus arrival time and depth before pulse compres-
896 sion produced by a point source at 800 m depth with the 75
897 Hz carrier frequency emitting a phase-modulated m -sequence.
898 b) The wave field in (a) after pulse compression (matched fil-
899 tering). c) The mode 1 arrival of the mode-processed wave
900 field shown in (a). d) The mode 1 arrival after pulse compres-
901 sion. Note that the mode 1 arrival in (d) may be obtained
902 either by pulse compression of the mode 1 arrival in (c), or by
903 mode filtering of the wave field in (b). The mode filtering was
904 performed with a long and dense array sufficient to resolve all
905 propagating modes. 10

906	4	a) Modes 1, 2, and 3 computed at 37.5 Hz in the C0 profile.	
907		The domain of interest lies between 120 m and 1660 m (un-	
908		shaded area). b) Array configurations resulting in BERs of	
909		less than 1% with 80% probability, at all eight ranges simul-	
910		taneously up to 400 km, from processing of modes 1, 2, and	
911		3 with a simulated SNR=20 dB. c) Array configurations result-	
912		ing in BERs of less than 1% with 90% probability, at all	
913		eight ranges simultaneously up to 400 km, from processing of	
914		modes 1, 2, and 3 with a simulated SNR=20 dB. d) Same as	
915		panel (b), but with BERs of less than 5% at ten ranges up to	
916		500 km. e) Same as panel (c), but with BERs of less than 5%	
917		at ten ranges up to 500 km. Note that the mode numbers are	
918		integers and the array configurations are offset horizontally	
919		from the integer marks for visualization purposes.	11
920	5	The number of hydrophones required to achieve either BERs of	
921		less than 1% at ranges up to 400 km or BERs of less than 5%	
922		at ranges up to 500 km with 80% probability by processing modes	
923		1-3 for various SNRs. Sixty-three hydrophones are required to	
924		achieve BERs < 1% at $r \leq 400$ km by processing mode 3 with	
925		an SNR of 5 dB (not shown).	15
926	6	The waveguide invariant (β) dependence on frequency for modes	
927		19 and 20. The frequency bands within which $ \beta < 0.15$ are	
928		shown in bold. The source should be placed at a depth where	
929		it will excite modes at these frequencies. The estimated opti-	
930		mal source depth is 190 m.	17
931	7	a) Modes 19 and 20 computed at 37.5 Hz in the C1 profile.	
932		The domain of interest is between the ocean surface and 3400	
933		m depth. b-e) Arrays that resulted in BERs not exceeding a	
934		given threshold (1% or 5%) at ranges up to 400 km or 500 km	
935		with respective probabilities. These panels are constructed	
936		similarly to Figures 4b)-4e).	18
937	8	The number of hydrophones required to achieve either BERs	
938		of less than 1% at ranges up to 400 km or BERs of less than 5%	
939		at ranges up to 500 km with 50% probability using processing	
940		of modes 19 and 20 for various SNRs. One hundred and fifty-	
941		eight hydrophones are required to achieve BERs < 5% at $r \leq$	
942		500 km by processing mode 19 with an SNR of 5 dB (not shown).	19

943 9 Estimating hydrophone depth for low BERs. a) Mode 1 in the
944 C0 profile at 75 Hz. b) Depth estimates for two-hydrophone
945 arrays that resulted in BERs of less than 1% with an SNR of
946 10 dB and a probability of 90%. c) Mode 20 in the C1 profile
947 at 75 Hz. d) Depth estimates for four-hydrophone arrays that
948 resulted in BERs of less than 1% for an SNR of 10 dB and a
949 probability of 50%. Corresponding mode rays are shown by
950 solid lines. The depths of mode rays at the discrete ranges of
951 interest are shown by black dots. 22

952 10 An example of phase errors from two-hydrophone array pro-
953 cessing for mode 1 (top panel) and four-hydrophone array pro-
954 cessing for mode 20 (bottom panel) at 400 km range with an
955 SNR of 10 dB. The phase errors are shown with black solid
956 lines. The thick gray line is the idealized transmitted square
957 wave (with unit amplitude). The black dots show the digits
958 recovered from the phase function. The horizontal axis is the
959 absolute arrival time. The vertical axis on each panel shows
960 phase errors between $-\pi$ and π 24